International Journal of Engineering

Centralized Path Planning for Multi-aircraft in the Presence of Static and Moving Obstacles

M. Mirzaei Teshnizi[a], A. Kosari*[a], S. Goliaei[a], S. Shakhesi[b]

[a] Faculty of New Science and Technology, University of Tehran, Tehran, Iran
[b] Faculty of Iranian Space Research Center, Tehran, Iran

A B S T R A C T

This article proposes a new approach for centralized path planning of multiple aircraft in presence of the obstacle-laden environment under low flying rules. The problem considers as a unified nonlinear constraint optimization problem. The minimum time and control investigate as the cost functions and the maximum velocity and power consider as the constraints. The pseudospectral method applies as a popular and fast direct method to solve the constrained path planning problem. The three-degree-of-freedom nonlinear point mass equations of motion with realistic operational aircraft constraints consider through the simplified mathematical model. The fixed obstacle considers as a combination of spheres with different radius. Also, the moving obstacles consider as a sphere with a known radius and fly at a constant speed. The effectiveness of the proposed concept will be demonstrated by presenting four case studies with a different number of aircraft along with the static and moving obstacles in various scenarios to ensure safe and effective flights.

doi: 10.5829/ije.2020.33.05b.25

1. INTRODUCTION

The concept of point-to-point Urban Air Transportation (UAT) is growing fast. The large cities with traffic congestion problems have stepped forward to start air transportation such as Dubai, Los Angeles, Rio de Janeiro, and Sydney [1]. Besides, several companies try to build operational vehicles, which can fly in the urban environment, Volocopter VC200, Lilium Jet, Uber air taxi, City Airbus, and Ehang184 are such projects, see Figure 1 [2]. Notwithstanding, the manufacturing and technological development, there are other challenges in air traffic management, air space regulations, and certification. As a regulation and certification perspective, the Federal Aviation Administration (FAA) and European Aviation Safety Agency (EASA) are responsible for discussing the requirements and licenses for this autonomous or piloted concept [3–5]. For carrying passengers in the dynamic environment by the UAT need a more intelligent Air Traffic Management System

(ATMS). According to civil aviation "Air-taxiing means flight by a helicopter, or other types of aircraft capable of vertical takeoff and landing, above the surface of an aerodrome at a ground speed of fewer than 20 knots to taxi under normal aviation practice" [6].

The concept of point to point transportation means that the aircraft must fly from an origin to the destination. During the flight, each one doesn't allow to fly in part of the airspace due to urban airspace limitation, which encompasses prohibited areas, restricted areas, military operations areas, buildings, etc. [7, 8]. Also, these aircraft should avoid collisions with other aircraft on their path. The collision defines as: "Two or more aircraft lose minimum separation from each other" [7]. The important problem in real flight trajectories is that the aircraft dynamic and performance constraints should consider in the path planning [8, 9]. In practice, there are acceptable bounds related to the states and the control inputs (e.g., maximum thrust, maximum velocity). All of the mentioned limitations and considerations should model as

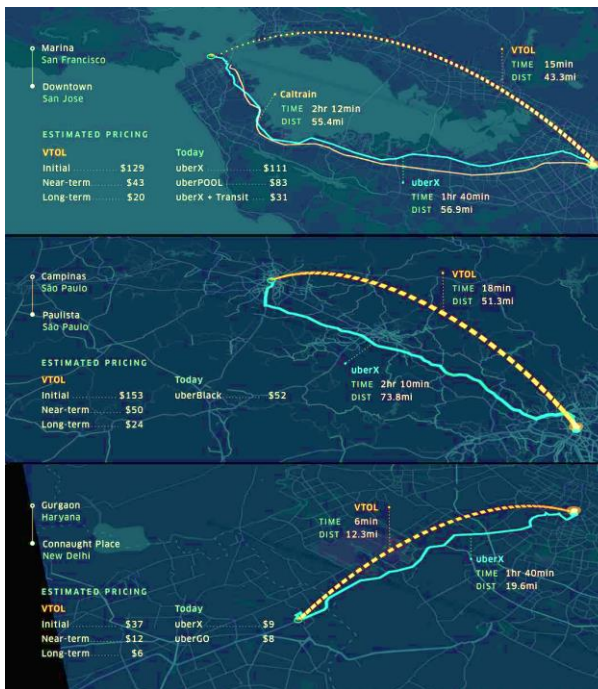*Corresponding Author Institutional Email: kosari_a@ut.ac.ir (A. Kosari)*

Figure 1. Comparison between urban air taxi and conventional urban transportation [2]

constraints to be respect in the aircraft flight path. As shown later, this problem converts to a nonlinear optimal control problem with constraints on the state and control variables. Solving the nonlinear optimal control problem requires the approximation of three types of mathematical elements: the integration in the cost function, the differential equation of motion, and the state-control constraints [10]. These requirements make Pseudospectral methods ideal as they are efficient for the approximation of all three mathematical elements [11–13].

The requirements, the certification process, and the safety of UAT investigated in literature [9]. The UAT marketing, travel time, motion efficiency and air traffic control mentioned as challenging topics in literature [14]. The hybrid model of air traffic control and management considering eight critical factors in ATMS proposed by Ma and Wu [15]. Based on the results, the performance of ATMS improved by desirable safety separation, the ATC structure, and collaborative decision-making. The performance characteristics of centralized and decentralized ATC analyzed in literature [16]. This paper indicated that the mitigation of the domino effect was an important factor in the design of ATMS and the centralized ATMS prevent the domino effect [16]. Also, collaborative decision making applied in the ATMS in the terminal area of Sao Paulo [17]. In other research, the optimal conflict resolution of air traffic (AT) developed in literature [18]. In this research, aircraft assumed to cruise in a horizontal plane with the constant velocity. The path planning methods, such as gradient descent, rapidly-

explore random tree, and numerical optimization methods thoroughly investigated for various collision-free path planning [19, 20]. The efficiency of the mixed-integer linear programming, dynamic sparse A*, and artificial potential fields investigated for the unmanned aerial vehicle collision avoidance [21]. Recently, several works focused extensively on the optimization approaches for computing collision-free aircraft trajectories with speed or heading control or both simultaneously [22–24]. The problem of path planning solved for a civilian aircraft in the presence of static obstacles with the online optimization direct multiple shooting method [25, 26]. In the current paper, the problem of the path planning for multi-aircraft in urban airspace with the operational and safety requirements will be considered in the presence of static and moving obstacles.

The trajectory optimization with nonlinear constraints needs an accurate numerical solution, cause there is no analytical solution or it is difficult to compute. Over the last decade, pseudospectral have risen to prominence in the numerical solution of trajectory optimization [27]. By this method, the unsolvable nonlinear optimal problem converts to a nonlinear programming problem that is much easier to solve. The conflict resolution between multi-aircraft in the conflict zone solved with these methods [26]. In this article, the conflict-free trajectory computed based on the summation of the aircraft velocity during the flight in obstacle-free airspace. More details and the key theoretical results reviewed in literature [28–30]. The present paper deals with solving the conflict-free path in the presence of static and moving obstacles by pseudospectral in a unified optimization problem in contrast to the mentioned works.

The rest of this paper is organized as follows. Section 2 presents the mathematical aircraft dynamics, obstacles, and definitions of the collision. The optimal control and problem formulation describe in Section 3. Simulation results based on the proposed approach with four case studies provide in Section 4. Some concluding remarks and the suggestions for future researches give in Section 5.

2. MATHEMATICAL MODELING

In this section, first, the dynamic model of the aircraft (air taxi) is provided. Then, the mathematical forms of the static and dynamic obstacles model to employ in the optimal control formulation as the state constraints. The path planning problem with obstacle and collision avoidance will define based on the low altitude flying rules. The optimal solution will be obtained with nonlinear mathematical models.

2. 1. Dynamic Model   In this paper, the point-mass model of the flying vehicle is used to describe the motion of the aircraft [26]. This model captures most of

the dynamical effects, encountered in the trajectory optimization problem, discussed in the literature. The three-degree-of-freedom (3DOF) model assumes a flat nonrotating system as an inertial coordinate frame with constant mass. Under these assumptions, aircraft equations of motion can be described as follows [26]:

$$\dot{x}_i = V_i \cos(\gamma_i)\cos(\chi_i) \tag{1}$$

$$\dot{y}_i = V_i \cos(\gamma_i)\sin(\chi_i) \tag{2}$$

$$\dot{h}_i = V_i \sin(\gamma_i) \tag{3}$$

$$\dot{V}_i = \frac{(T_i - D_i)}{m_i} - g\sin(\gamma_i) \tag{4}$$

$$\dot{\gamma}_i = \frac{(L_i \cos(\varphi_i) - m_i g \cos(\gamma_i))}{m_i V_i} \tag{5}$$

$$\dot{\chi}_i = \frac{L_i \sin(\varphi_i)}{m_i V_i \cos(\gamma_i)} \tag{6}$$

where $i = 1, 2 \ldots N$ is the number of aircraft, x_i is the down-range displacement, y_i is the cross-range displacement, h_i is the altitude, V_i is the ground speed that is assumed to be equal to airspeed, γ_i is the flight path angle, χ_i is the heading angle, m_i is the aircraft mass, which is assumed to be constant (electrical powered) and g is the acceleration due to gravity, L_i and D_i are the aerodynamic forces of lift and drag, respectively. The state vector is $X_i \triangleq [x_i, y_i, h_i, V_i, \gamma_i, \chi_i]$ and the control input vector is $U \triangleq [\varphi_i, n_i, T_i]$ as shown in Figure 2. Three control variables are the bank angle φ_i, the engine thrust T_i and the load factor n_i. The aircraft model should include the appropriate performance, physical and structural limitations of the aircraft. Any optimized trajectories that are planned can also include additional constraints related to the safety of passengers [6]. The following state-input constraints can be taken into account with lower and upper bounds [31, 32]:

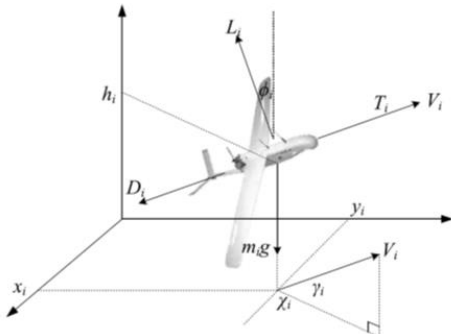$$X_{i_L} \leq X_i \leq X_{i_U} \qquad U_{i_L} \leq U_i \leq U_{i_U} \tag{7}$$

Figure 2. Aircraft and reference coordinate systems [26]

It can be shown that the system of nonlinear equations of motion (Equations(1)-(6)) can be transformed into an alternative form by defining the three virtual control variables as follows [32]:

$$\ddot{x} = U_1, \quad \ddot{y} = U_2, \quad \ddot{h} = U_3, \tag{8}$$

where U_1, U_2, and U_3 are virtual control variables. These virtual and actual control variables are related through the following equations [32]:

$$\varphi = a\tan\left(\frac{U_2 \cos\chi - U_1 \sin\chi}{\cos\gamma(U_3 + g) - \sin\gamma(U_1 \cos\chi + U_2 \sin\chi)}\right) \tag{9}$$

$$n = \left(\frac{\cos\gamma(U_3 + g) - \sin\gamma(U_1 \cos\chi + U_2 \sin\chi)}{g\cos\varphi}\right) \tag{10}$$

$$T = (\sin\gamma(U_3 + g) + \cos\gamma(U_1 \cos\chi + U_2 \sin\chi))m + D \tag{11}$$

$$\tan\chi = \frac{\dot{y}}{\dot{x}} \tag{12}$$

$$\sin\gamma = \frac{\dot{h}}{V} \tag{13}$$

The reduced aircraft models can be also expressed as follows [32]:

$$\dot{X}_i = AX_i + BU_i$$
$$p_i = C_p X_i$$
$$v_i = C_v X_i \tag{14}$$
$$A = \begin{bmatrix} 0 & 1 \\ 0 & 0 \end{bmatrix} \otimes I_3, \quad B = \begin{bmatrix} 0 \\ 1 \end{bmatrix} \otimes I_3$$
$$C_p = \begin{bmatrix} 1 & 0 \end{bmatrix} \otimes I_3, \quad C_v = \begin{bmatrix} 0 & 1 \end{bmatrix} \otimes I_3$$

where $X_i = [p^T{}_i, v^T{}_i]^T$ is the state vector, $p_i = [x_i, y_i, h_i]^T$ is the position, $v_i = [\dot{x}_i, \dot{y}_i, \dot{h}_i]^T$ is the velocity, $U_i = [u^T{}_{x_i}, u^T{}_{y_i}, u^T{}_{h_i}]^T$ is the virtual control, $I_3 \in R^3$ is the identity matrix, and $\otimes$ is the Kronecker product. The latter form is useful for mapping geometric trajectory parameters in terms of the aircraft control variables and vice versa. Such mappings are useful for efficient implementation of control constraints and simplification of the computational procedure [31–33].

2. 2. Low Altitude Flying Rules and Collision Model
UAT must be safe, efficient, predictable, and has a minimum impact on urban airspace. So UAT shall comply with the prohibitions under low altitude flying rules as represented in literature [6]. One of the prohibitions is the minimum safety distances between two aircraft and between aircraft and obstacle. For this purpose, aircraft has located at the center of a virtual sphere as a safety zone. The static obstacles have considered by a combination of the multiple spheres. The dynamic obstacle has modeled with a moving sphere. In

this article, the radius of the safety sphere is 600 meters. The collision or loss of separation has occurred whenever two safety sphere overlaps. There is a great amount of research in this area [21, 34, 35] and a comprehensive survey represented in literature [36].

2. 3. Aircraft Collision Model   Assume that $(x_i(t), y_i(t), z_i(t))$ is the position of the ith aircraft at time t. A conflict between the flying trajectories of the aircraft, i and j do not occur if the following relation is satisfied for all of the time:

$$\left(x_i(t) - x_j(t)\right)^2 + \left(y_i(t) - y_j(t)\right)^2 + \left(h_i(t) - h_j(t)\right)^2 \geq D^2 \tag{15}$$

D is the minimum separation safety radius. In addition, it is assumed that at time t=0, there exists a sufficient separation between all aircraft, so no collision occurs at the initial time.

2. 4. Obstacles Collision Model   The aircraft trajectory must be avoided from any obstacle such as terrain, restricted area, danger zone or any urban obstacle. The boundary of any obstacle can be defined by $\phi(x,y,h)$, so the allowed area will be as follows:

$$O_{free} = \{(x, y, h) \in R^3, \phi(x, y, h) \geq 0\} \tag{16}$$

If the obstacle moves with time, then:

$$O_{free} = \{(x, y, h) \in R^3, \phi(x(t), y(t), h(t)) \geq 0\} \tag{17}$$

In this paper, all obstacles considered as a combination of the multi sphere with a predefined radius as shown in Figure 3. It is important to note that the combination of multi-sphere can make different shapes.

3. OPTIMAL CONTROL AND TRAJECTORY PLANNING

The general form of the trajectory optimization for multi-aircraft can be formulated as follows [26]:
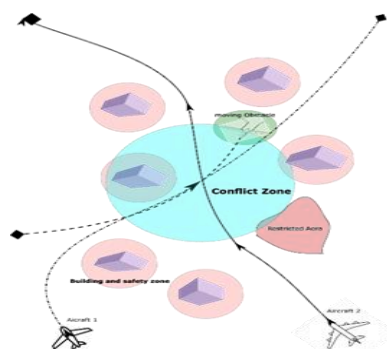

Figure 3. Aircraft in urban airspace with the static and moving obstacles

$$min J = \sum_{i=1}^{N} \int_{t_0}^{t_{f_i}} g(\boldsymbol{X}_i(t), \boldsymbol{U}_i(t), t) dt_i \tag{18}$$

$$subject. to: \frac{d}{dt} \boldsymbol{X}_i = f(\boldsymbol{X}_i, \boldsymbol{U}_i), \qquad i = 1 \dots N \tag{19}$$

$$C_{ineq}(\boldsymbol{X}_i(t), \boldsymbol{U}_i(t)) \geq 0 \tag{20}$$

$$\boldsymbol{X}_i^L(t) \leq \boldsymbol{X}_i(t) \leq \boldsymbol{X}_i^U(t) \tag{21}$$

$$\boldsymbol{U}_i^L(t) \leq \boldsymbol{U}_i(t) \leq \boldsymbol{U}_i^U(t) \tag{22}$$

where g is the integral cost functions, $\boldsymbol{X}_i$ represent algebraic state vector, and $\boldsymbol{U}_i$ is the control vector, $i = 1 \dots N$ represents the index of aircraft, t_0, t_{f_i} represent the initial and terminal time, $C_{ineq}()$ represents inequality constraints such as collision avoidance and minimum separation Equations (15)-(16). Obviously, the lower and upper bound on the state and control vector can be considered as linear inequality constraints. In general, such dynamic optimization problems cannot be solved analytically [37]. Most practical problems are solved using nonlinear programming methods based on some discretization of the original continuous control problem [20, 27]. In this paper, the pseudospectral method used for solving the optimal control problem with constraints with bounded inputs and state variables. For the integration in the cost function, the differential equation, and the state-control constraints, pseudospectral methods are efficient for the approximation of all three mathematical objects. Pseudospectral methods are a class of direct collocation methods where the optimal control problem is transcribed to a nonlinear programming problem (NLP) by parameterizing the state and the control using global polynomials and collocating the differential-algebraic equations using nodes obtained from a Gauss-quadrature [29].

3. 1. Pseudospectral Method for Optimal Path Planning   This method is based on approximation of the nonlinear optimization problem using interpolating polynomials in collocation points that are defined as the roots of the Kth degree Legendre polynomial. Without loss of generality, the time interval $t \in [t_0, t_f]$ can be transformed into $\tau \in [-1,1]$ by the change of variable [29].

$$t = \frac{1 + \tau}{1 - \tau} \tag{23}$$

The basic idea of pseudospectral methods is to approximate $\boldsymbol{X}(\tau)$ by K^{th} order polynomial $\boldsymbol{X}(\tau_K)$ based on Lagrange interpolation of their values at the LG node point. Let $(\boldsymbol{X}(\tau_l), U(\tau_l))$, be an approximation of a feasible solution $(\boldsymbol{X}(\tau), U(\tau))$ evaluated at the node τ_l then the state and control vectors are approximated as follows [29]:

$$\mathbf{X}(\tau) \approx X(\tau) = \sum_{l=0}^{K} X(\tau_l). \prod_{m=0 m \neq l}^{K} \frac{\tau - \tau_m}{\tau_l - \tau_l} =$$
$$\sum_{l=0}^{K} X(\tau_l). L_l(\tau) \tag{24}$$

$$\mathbf{U}(\tau) \approx U(\tau) = \sum_{l=1}^{K} U(\tau_l). \prod_{m=1, m \neq l}^{K} \frac{\tau - \tau_m}{\tau_l - \tau_m} =$$
$$\sum_{l=1}^{K} U(\tau_l). L^*_l(\tau) \tag{25}$$

The derivative of the series (24) and evaluating at the lth collocation point, τ_l, gives:

$$\dot{\mathbf{X}}(\tau) \approx \dot{X}(\tau) = \sum_{i=0}^{K} X(\tau_i). \dot{L}_i(\tau)$$
$$D_{ri} = \dot{L}_r(\tau_i), (r = 1, ... K), (i = 0, ... K) \tag{26}$$

where D_{ri} is the $K \times (K+1)$ pseudospectral differentiation matrix. The dynamic constraint (19) is then collocated at the LG points as follows [29]:

$$\sum_{i=0}^{K} D_{ri} X_i - \frac{t_f - t_0}{2} f(X_r, U_r, \tau_r; t_0, t_f) = 0,$$
$$f(X_r, U_r, \tau_r; t_0, t_f) \equiv f_r \tag{27}$$
$$(r = 1, ... K)$$

where $X_r = X(\tau_r) \in R^n, U_r = U(\tau_r) \in R^m$. The differential dynamic constraint (19) is transcribed into algebraic constraint via Equation (27). Note that the dynamic constraint is collocated only at the LG points, whereas the state is approximated at the N LG points plus the terminal point [38]. Moreover, the initial condition is $X_0 = X(-1)$ and the final condition X_f by the fundamental theorem of calculus is defined as follows:

$$X_f \equiv X_0 + \frac{t_f - t_0}{2} \sum_{i=1}^{K} \omega_i f_i \tag{28-a}$$

$$\omega_i = \frac{2}{K(K+1)}. \frac{1}{[L(\tau_l)]^2} \tag{28-b}$$

where ω_i are the LG weights.

Thus the continuous cost function of Equation (18) is approximated by the Gauss quadrature integration rule as follows:

$$j_m = \left(\frac{t_{fm} - t_0}{2} \sum_{i=1}^{K} \omega_{im} g_{im}(X_{im}, U_{im}, \tau_{im}; t_0, t_{f_j})\right),$$
$$m = 1 ... N \tag{29}$$

In addition, the path constraint (20) is discretized as follows:

$$C_{ineq_j}\left(\mathbf{X}_j(\tau_i), \mathbf{U}_j(\tau_i)\right) \geq 0 \tag{30}$$

The cost function of Equation (29) along with the algebraic constraints of Equation (27) and the discretized inequality Equation (30) with the boundary condition Equation (28) defines an NLP whose solution is an approximate solution to the continuous nonlinear optimization problem in Equations (18)-(20).

3. 2. First-order Optimal Condition

The first-order optimality conditions (Karush–Kuhn–Tucker condition KKT) of the NLP become a discretization of the first-order optimality conditions for the continuous control problem Equations (18)-(20). The KKT condition can be formulated using the Lagrangian multipliers $\Lambda_r \in \mathbf{R}^n, \mu_r \in \mathbf{R}^c, r = 1, ..., K$ and $\Lambda_F \in \mathbf{R}^n$ as [38]:

$$J_a = \frac{t_f - t_0}{2} \sum_{r=1}^{K} \omega_r g_r - \sum_{r=1}^{K} \tilde{\mu}_r^T C_r$$
$$- \sum_{r=1}^{K} \tilde{\Lambda}_r^T \left(\sum_{r=1}^{K} D_{ri} X_i - \frac{t_f - t_0}{2} f_r\right) \tag{31}$$
$$- \tilde{\Lambda}_F^T \left(X_f - X_0 - \frac{t_f - t_0}{2} \sum_{r=1}^{K} \omega_r f_r\right)$$

where J_a is the augmented cost function. The first-order optimality conditions are obtained by setting equal to zero of the derivative of the augmented cost function with respect to $X_r, U_r, \tilde{\mu}_r, \tilde{\Lambda}_r, \tilde{\Lambda}_F, t_0$, and t_f. The solution to the NLP of the previous section must satisfy the following conditions [38]:

$$\sum_{r=1}^{K} D_{ri} X_i = \frac{t_f - t_0}{2} f_r \tag{32}$$

$$\frac{\partial}{\partial X_r}\left(\frac{t_f - t_0}{2} \sum_{r=1}^{K} \omega_r g_r\right) = \frac{\partial}{\partial X_r}\left(\sum_{r=1}^{K} \tilde{\mu}_r^T C_r\right) +$$
$$+ \frac{\partial}{\partial X_r}\left(\sum_{r=1}^{K} \tilde{\Lambda}_r^T \left(\sum_{r=1}^{K} D_{ri} X_i - \frac{t_f - t_0}{2} f_r\right)\right) \tag{33}$$
$$- \frac{\partial}{\partial X_r}\left(\tilde{\Lambda}_F^T \left(\frac{t_f - t_0}{2} \sum_{r=1}^{K} \omega_r f_r\right)\right)$$

$$\frac{\partial}{\partial U_r}\left(\frac{t_f - t_0}{2} \sum_{r=1}^{K} \omega_r g_r\right) = \frac{\partial}{\partial U_r}\left(\sum_{r=1}^{K} \tilde{\mu}_r^T C_r\right)$$
$$+ \frac{\partial}{\partial U_r}\left(\sum_{r=1}^{K} \tilde{\Lambda}_r^T \left(\sum_{r=1}^{K} D_{ri} X_i - \frac{t_f - t_0}{2} f_r\right)\right) \tag{34}$$
$$- \frac{\partial}{\partial U_r}\left(\tilde{\Lambda}_F^T \left(\frac{t_f - t_0}{2} \sum_{r=1}^{K} \omega_r f_r\right)\right)$$

$$\frac{\partial}{\partial t_0}\left(\frac{t_f - t_0}{2} \sum_{r=1}^{K} \omega_r g_r\right) = + \frac{\partial}{\partial t_0}\left(\sum_{r=1}^{K} \tilde{\mu}^T_r C_r\right)$$
$$+ \frac{\partial}{\partial t_0}\left(\sum_{r=1}^{K} \tilde{\Lambda}^T_r \left(\frac{t_f - t_0}{2} f_r\right)\right) \tag{35}$$
$$- \frac{\partial}{\partial t_0}\left(\tilde{\Lambda}^T_F \left(\frac{t_f - t_0}{2} \sum_{r=1}^{K} \omega_r f_r\right)\right)$$

$$\frac{\partial}{\partial t_f}\left(\frac{t_f - t_0}{2} \sum_{r=1}^{K} \omega_r g_r\right) = + \frac{\partial}{\partial t_f}\left(\sum_{r=1}^{K} \tilde{\mu}^T_r C_r\right)$$
$$+ \frac{\partial}{\partial t_f}\left(\sum_{r=1}^{K} \tilde{\Lambda}^T_r \left(\frac{t_f - t_0}{2} f_r\right)\right) \tag{36}$$
$$- \frac{\partial}{\partial t_f}\left(\tilde{\Lambda}^T_F \left(\frac{t_f - t_0}{2} \sum_{r=1}^{K} \omega_r f_r\right)\right)$$

$$C_r \leq 0 \rightarrow \begin{cases} C_{jr} < 0 \rightarrow \tilde{\mu}_{jr} = 0 \\ C_{jr} = 0 \rightarrow \tilde{\mu}_{jr} \leq 0 \end{cases} \tag{37}$$

$$X_f - X_0 = \frac{t_f - t_0}{2} \sum_{r=1}^{K} \omega_r f_r \tag{38}$$

$$\tilde{\Lambda}_F = -\frac{\partial}{X_r}\left(\frac{t_f-t_0}{2}\right)\sum_{r=1}^K \omega_r\, g_r + \sum_{r=1}^K \tilde{\mu}^T{}_r\, C_r$$
$$-\sum_{r=1}^K \tilde{\Lambda}^T{}_r \left(\frac{t_f-t_0}{2}f_r\right) - \tilde{\Lambda}^T_F\left(-\frac{t_f-t_0}{2}\sum_{r=1}^K \omega_r\, f_r\right) \tag{39}$$

Theorem 1. The first-order optimality conditions (Equations (31)-(39)) of the NLP are equivalent to the pseudospectral discretized form of the continuous first-order necessary conditions of the continuous optimization problem (Equations (28)-(30)) [11]. Furthermore, a costate estimate can be found from Lagrangian multipliers [11, 30].

Theorem 1 represents that solving the NLP is equivalent to applying the pseudospectral discretization to the first-order necessary condition of the continuous optimization problem.

3. 3. Problem Formulation   The total flight time and control effort can be considered as two important factors in path planning and conflict resolution. In this paper, both of time and control efforts are investigated. The problem is formulated as follows:
The system dynamic:

$$\dot{X} = AX + BU$$
$$X = [X_1^T, \ldots, X_N^T]^T$$
$$U = [U_1^T, \ldots, U_N^T]^T$$
$$A = \begin{bmatrix} A_1 & 0_{6\times6} & \cdots & 0_{6\times6} \\ 0_{6\times6} & A_2 & \cdots & \vdots \\ \vdots & 0_{6\times6} & \ddots & 0_{6\times6} \\ 0_{6\times6} & \cdots & 0_{6\times6} & A_N \end{bmatrix},$$
$$A_i = \begin{bmatrix} 0_{3\times3} & 0_{3\times3} \\ 0_{3\times3} & I_{3\times3} \end{bmatrix}$$
$$BU = \begin{bmatrix} bu_1 \\ \vdots \\ bu_N \end{bmatrix}, bu_i = \begin{bmatrix} 0_{3\times1} \\ u_i \end{bmatrix}, i = 1\ldots N \tag{40}$$

where N is the number of aircraft.
The cost functions:

$$j = \int d\tau \quad or \quad \int U^2(\tau_l)d\tau \tag{41}$$

The deconfiliction constraints:

$$C_{ineq} = C_{ij} = C_{ji} = \|p_i(\tau_l) - p_j(\tau_l)\| \geq R_s,$$
$$i \neq j, l = 1\ldots K$$
$$p_i = X[6\times(i-1)+1:6\times(i-1)+3], i = 1\ldots N$$
$$p_j = X[6\times(j-1)+1:6\times(j-1)+3], j = 1\ldots N \tag{42}$$

Static obstacle avoidance:

$$R_{SO} - \|X_i(\tau_m; 0:t_f) - P_{SO}\| \leq 0, i = 1\ldots N \tag{43}$$

P_{SO} is the position of the static obstacle. For simplicity, each obstacle is modeled by a combination of multiple spheres with a different radius.

Moving obstacle avoidance:

$$R_{MO} - \|X_i(\tau_m; 0:t_f) - P_{MO}(\tau_m; 0:t_f)\| \leq 0, i = 1\ldots N \tag{44}$$

P_{MO} is the position of moving obstacle and model.
The pure state constraint (maximum velocity):

$$V_i(\tau_m; 0:t_f) \leq V_{i_{max}} \tag{45}$$

The control constraint (maximum power):

$$m_i \times \|U_i(\tau_m; 0:t_f)\| \times V_i(\tau_m; 0:t_f) \leq P_{i_{max}} \tag{46}$$

where m_i is the mass of aircraft.
The proposed approach can be represented by the following diagram, Figure 4.

4. CASE STUDIES AND NUMERICAL RESULTS

This section presents the numerical simulation for a formation flight trajectory planning problem in urban airspace. The optimal collision-free trajectories compute by utilizing the pseudospectral method. The centralized conflict resolution problem solved without static and moving obstacles [38].

The current research solves the conflict-free path in the presence of static and moving obstacles. The performance parameters of the electric Vertical Take-Off and Landing (eVTOL) Lilium Jets (henceforth called A/C) use for this simulation. A/C is powered by 36 ducted electric fan engines, which generate approximately 320kW (435hp) of power and has a range of 300km, with the maximum altitude about 4km and a maximum speed about of 85m/s [39]. Its take-off weight is 400kg. Four
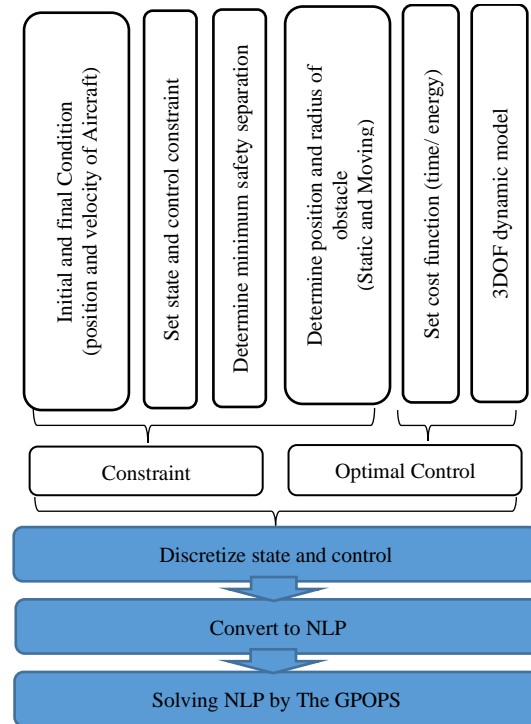

Figure 4. Diagram for Pseudospectral method

scenarios represent the effectiveness of the proposed approach under the following conditions:

- Airspace dimension: (900×900×400) meters.
- The minimum safety separation: 60 meters.
- The static and moving obstacles and surrounding safety zone are modeled as a sphere with the predefined radius (100, 90, 80, 70, 60, 50 meters)
- Take-off and landing phases are omitted.
- Maximum speed 85m/s.
- Maximum available power for each A/C equal to 320kW

So, the simulation can be considered as a part of the real flight in the low altitude urban airspace.

Case 1. In this case, the UAV flies over the urban airspace with one-static obstacles in either minimum time or minimum energy form as the performance index. Table 1 shows the parameters used in the simulation.

Although this case is not likely to happen in reality, this case shows the ability of the algorithm to solve nonlinear constrained optimal control. This algorithm has robust and fast convergence to the optimal solution as shown in Figure 5. Obviously, the control effort in the minimum time is much more than the minimum energy as shown in Table 2. Since the minimum energy is obtained in infinite time, the simulation time has been considered as high enough. Base on the company policy and/or passenger request, one of the strategies (time/ energy) can be chosen.

Case 2. In this case, A/C flies over the urban airspace in the presence of one static obstacle and one moving obstacle in either minimum time or minimum energy scenario. The simulation parameters are similar to the previous case as summarized in Table 1 with a moving obstacle is considered with the velocity vector $V_0=[10, 10, 0]$ (m/s) and the initial position $Z_0=[0, 0, 100]$ (m).

TABLE 1. Parameters for numerical simulation case 1

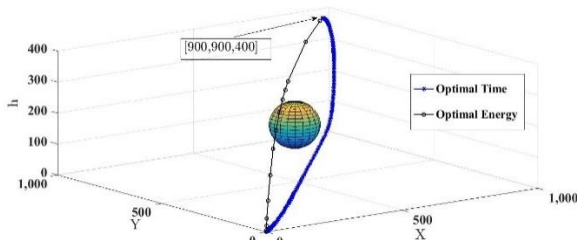| Parameter description	Value (meter)
Initial position	[0, 0, 0]
Final position	[900, 900, 400]
Center of obstacle	[450, 450, 200]
Radius of obstacle	100

Figure 5. The optimal trajectory for A/C in the presence of one static obstacle -minimum time and minimum energy

TABLE 2. Results of minimum time and minimum energy case 1

Performance Index	Flight time duration (s)	Control effort (m²/s³)	Run time (s)
$J = \int dt$	22.58	250.56	0.4
$J = \int u^2\, dt, t_f = 500s$	500	8.31	0.43

In this case, the effect of the moving obstacle with on the flight time and control effort has been investigated as shown in Figure 6. As expected, time and control effort increased, as shown in Table 3. The increase in time and control effort in minimum time is more than in minimum energy. In other words, the impact of disturbance (moving obstacle) on minimum time is greater than minimum energy.

Case 3. In this case, A/C flies over the urban airspace in the presence of six static obstacles and two moving obstacles in either the minimum time or the minimum energy form as the cost function. The position and radius of obstacles are presented in Table 4.

In this case, path planning of A/C considering multiple static and moving obstacles has been investigated as shown in Figure 7. As the number of obstacles increases, the flight time and the control effort will be also increased as shown in Table 5.

Case 4. In this case, six A/Cs fly over the urban airspace in the presence of a combination of multi-sphere as static obstacles and two moving obstacles with constant speed. The combination of multi-sphere can generate different shapes for a realistic urban environment. The problem of multi-aircraft conflict resolution without considering static and moving obstacles investigated [37].
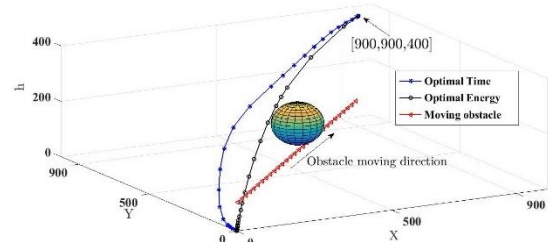

Figure 6. The optimal trajectory for A/C in the presence of one static obstacle and one moving obstacle -minimum time and minimum energy

TABLE 3. Results of minimum time and minimum energy case 2

Performance Index	Flight time duration (s)	Control effort (m²/s³)	Run time (s)
$J = \int dt$	24.1	264	0.69
$J = \int u^2\, dt, t_f = 500s$	500	8.36	0.8

TABLE 4. Parameters for numerical simulation case 3

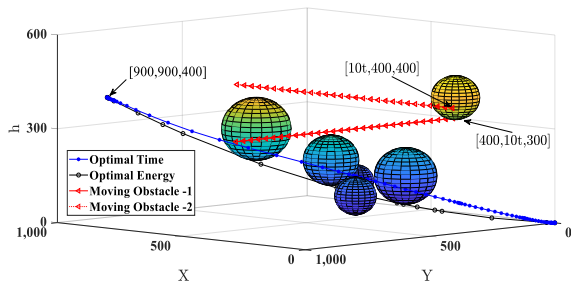| Parameter description	Value (meter)
Initial position	[0, 0, 0]
Final position	[900, 900, 400]
Center of obstacle 1, Radius	O1= [300,300,150] , R1=90
Center of obstacle 2, Radius	O2= [600,600,300] , R2=100
Center of obstacle 3, Radius	O3= [600,200,100] , R3=50
Center of obstacle 4, Radius	O4= [200,600,120] , R4=60
Center of obstacle 5, Radius	O5= [200,200,400] , R5=70
Center of obstacle 6, Radius	O6= [450,450,200] , R6=80
Moving obstacle 1 position	Mo1=[400, 10t, 300] , R =100
Moving obstacle 2 position	Mo2= [10t, 400, 400] , R =100

TABLE 5. Results of minimum time and minimum energy case 3

Performance Index	Flight time duration (s)	Control effort (m²/s³)	Run time (s)
$J = \int dt$	24.64	274.38	4.3
$J = \int u^2\, dt, t_f = 500s$	500	8.49	4.1

The aircraft initial and final position for case 4 are presented in Table 6. The comprehensive model for UAT has been investigated in case 4. The running time for minimum time and minimum energies are 152.2 and 156.8 seconds respectively.

TABLE 6. Aircraft initial and final position case 4

Aircraft	Initial position(m)	Final position(m)
A/C1	[100,0,400]	[900, 700, 0]
A/C2	[900,0,500]	[900, 900, 400]
A/C3	[0, 100, 0]	[200, 800, 0],
A/C4	[0, 0, 0]	[900,700,400],
A/C5	[600, 0, 0]	[0,900, 300],
A/C6	[800,0,0]	[0,900, 500]

Figure 7. The optimal trajectory for A/C in the presence of six static obstacles and two moving obstacles -minimum time and minimum energy

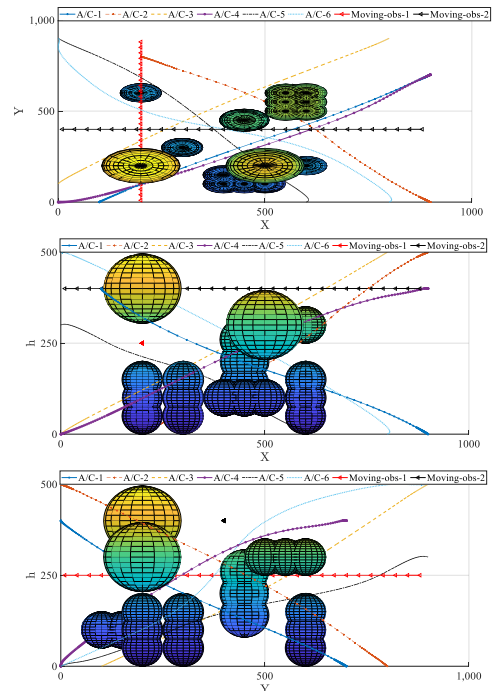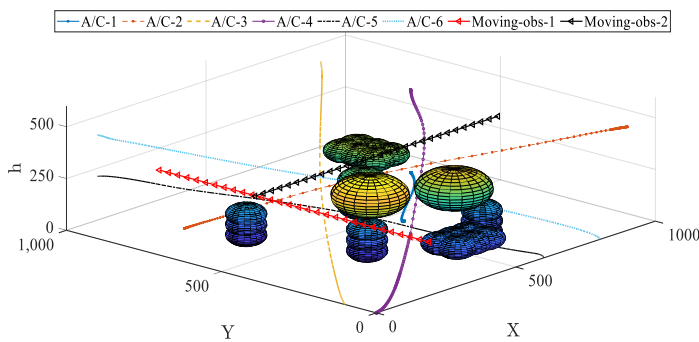The optimal path in the minimum time and minimum energy have been depicted in Figures 8 and 9,

Figure 8. The optimal trajectory for six A/Cs in the presence of multi-static obstacles and two moving obstacles- 3D-view (right side) – and the X-Y, X-h, Y-h view (left side) -minimum time approach
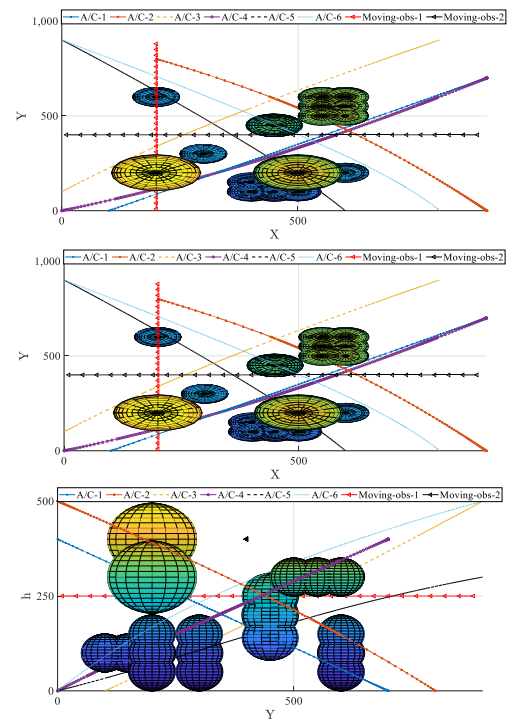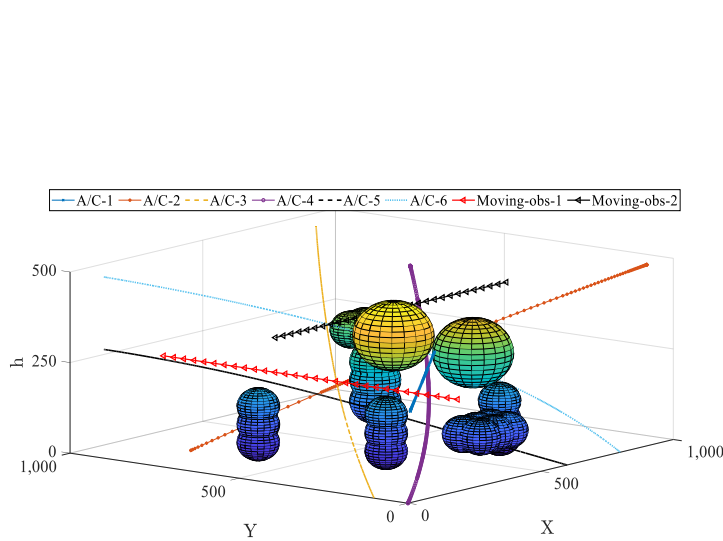
Figure 9. The optimal trajectory for six A/Cs in the presence of multi-static obstacles and two moving obstacles- 3D-view (right side) – and the X-Y, X-h, Y-h view (left side) -minimum energy approach

respectively. In the minimum time scenario, the time history of velocity is shown in Figure 10. As obviously, each A/C has restricted conditions regarding the allowable power and maximum velocity. In addition, the history of power and maximum allowable power are shown in Figure 11. The control effort (power history) has a sharp variation during the flight. On the other hand, in the minimum energy scenario, the history of velocity, and control efforts of each of A/Cs are depicted in Figures 12 and 13, respectively. The control effort (power history) has a smooth variation, as expected.

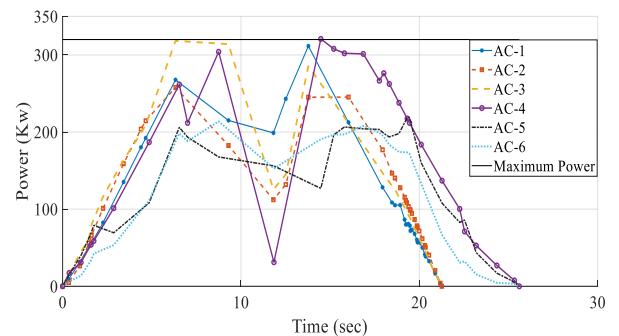The results of minimum time and minimum energy for case 4 are presented in Table 7.

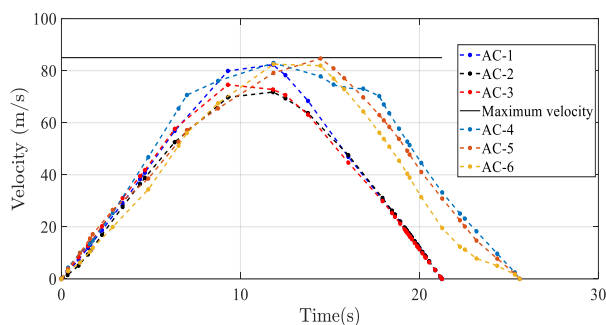**Figure 11.** History of power as a function of time -minimum time approach

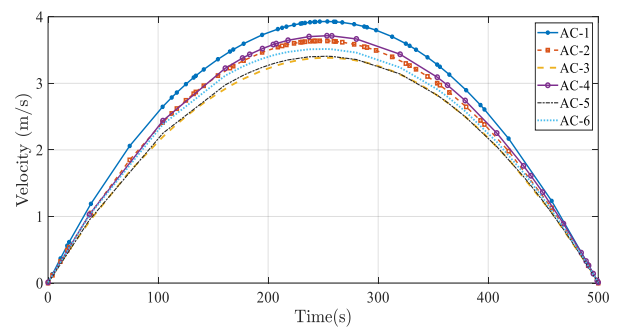**Figure 10.** History of A/C's velocity as a function of time - minimum time approach

Figure 12. History of velocity as a function of time -minimum energy approach
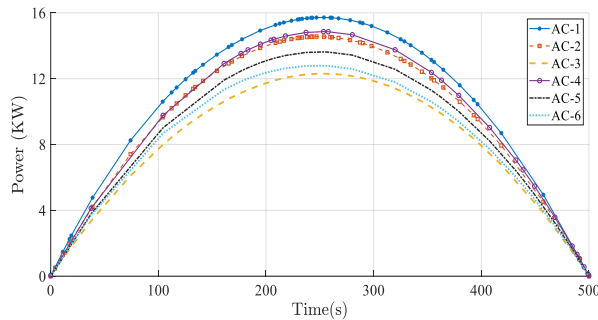
Figure 13. History of power as a function of time -minimum energy approach

TABLE 7. Results of minimum time and minimum energy case 4

Aircraft	Performance Index	Flight time duration (s)	Control effort (m²/s³)
A/C 1	Minimum time	21.2	330.1
	Minimum energy	500	8.67
A/C 2	Minimum time	21.18	334.2
	Minimum energy	500	8.72
A/C 3	Minimum time	21.12	334.5
	Minimum energy	500	8.61
A/C 4	Minimum time	25.68	351.5
	Minimum energy	500	9.16
A/C 5	Minimum time	25.50	349.8
	Minimum energy	500	9.01
A/C 6	Minimum time	25.53	349.9
	Minimum energy	500	8.95

5. CONCLUSION

This paper proposes an operational path planning for urban air transportation in the presence of static and moving obstacles. The methodology investigates the conflict-free path for multiple aircraft as an optimal control problem framework under low flying rules. LG pseudospectral method used to solve nonlinear optimization problems. The linearized point mass equations of motion in three-dimensional utilized to reduce computational complexity and the realistic operational constraints applied to the mathematical model. The static and moving obstacles modeled with a combination of spheres. The effectiveness of the proposed approach for solving the centralized trajectory optimization problem demonstrated by presenting four case studies. The minimum time and minimum control effort investigate as the cost functions and the maximum velocity and power consider as the state and control constraints with different obstacles.

The influence of the static and moving obstacles on the flight path investigated in these cases. As shown in results, each of A/C can fly in urban restricted airspace in an optimized conflict-free path. The computational load and running time increased with an increasing number of obstacles and A/C, so needs a more powerful computer for real case. The results indicate that the proposed approach is applicable in urban air transportation; thus, this method can employ to obtain the conflict-free path efficiently. However, one point with the proposed approach is that the centralized path planning and conflict resolution could rarely lead to a chain reaction of new-popped conflicts. Future research can dedicate to the complete flight with take-off and landing phases, or utilizing real urban airspace limitations and moving obstacles with variable speed. Besides, the cost function can be used as a combination of time and energy or flight cost per passenger.

6. REFERENCES

1. E. A. Munsif Vengattil, 9 May 2018. [Online]. Available: https://www.reuters.com/article/us-uber-elevate/uber-opens-up-international-contest-for-a-third-flying-taxi-city-idUSKBN1IA2TQ

2. M. Huber, Barrons, 10 May 2018. [Online]. Available: https://www.barrons.com/articles/uber-targets-los-angeles-as-next-air-taxi-market-1525965120

3. Federal Aviation Administration, 30 April 2020. [Online]. Available: https://www.ecfr.gov/cgi-bin/text-idx?c=ecfr&sid=4d87705808eddb6d1f536f86f59ff284&tpl=/ecfrbrowse/Title14/14cfr119_main_02.tpl

4. European Aviation Safety Agency,4 July 2018. [Online]. Available: https://www.easa.europa.eu/regulations

5. Part 135-Operating Requirements: Commuter and On-Demand Operations and Rules Governing Persons On Board Such Aircraft, Code of Federal Regulations, 2013. Available: https://www.gleim.com/aviation/faraim/index.php?componentNum=135

6. Civil Aviation (Rules of the Air) Regulations, (LN. 2014/256), 2014. http://citeseerx.ist.psu.edu/viewdoc/download?doi=10.1.1.730.5430&rep=rep1&type=pdf

7. Aeronautical Information Manual, U.S. Department of Transportation, Federal Aviation Regulations, 2018. https://www.sportys.com/media/pdf/eoc913.pdf

8. Kosari, A. and Teshnizi, M. M., "Optimal Trajectory Design for Conflict Resolution and Collision Avoidance of Flying Robots using Radau-Pseudo Spectral Approach", In 2018 6th RSI International Conference on Robotics and Mechatronics (IcRoM), IEEE, (2018), 82–87.

9. Fu, Y., Zhang, Y. and Yu, X., "An advanced sense and collision avoidance strategy for unmanned aerial vehicles in landing phase", *IEEE Aerospace and Electronic Systems Magazine*, Vol. 31, No. 9, (2016), 40–52.

10. Ghassemi, H., Sabetghadam, F. and Soltani, E., "A fast immersed boundary fourier pseudo-spectral method for simulation of the incompressible flows", *International Journal of Engineering - Transaction C: Aspects*, Vol. 27, No. 9, (2014), 1457–1466.

11. Gong, Q., Kang, W. and Ross, I. M., "A pseudospectral method for the optimal control of constrained feedback linearizable systems", *IEEE Transactions on Automatic Control*, Vol. 51, No. 7, (2006), 1115–1129.

12. Hesthaven, J.S., Gottlieb, S. and Gottlieb, D., Spectral methods for time-dependent problems, (Vol. 21), Cambridge University Press,

(2007).

13. Kanjanawanishkul, K., "Path following and velocity optimizing for an omnidirectional mobile robot", *International Journal of Engineering - Transaction A: Basics*, Vol. 28, No. 4, (2015), 537–545.

14. Holden, J. and Goel, N., Fast-forwarding to a future of on-demand urban air transportation, San Francisco, CA., (2016).

15. Ma, Y.F. and Wu, X. Y., "Evaluation of air traffic management system using a hybrid model", In 2016 IEEE International Conference on Industrial Engineering and Engineering Management (IEEM), IEEE, (2016), 1294–1298.

16. Krozel, J., Peters, M., Bilimoria, K.D., Lee, C. and Mitchell, J. S., "System performance characteristics of centralized and decentralized air traffic separation strategies", *Air Traffic Control Quarterly*, Vol. 9, No. 4, (2001), 311–332.

17. Jha, P., Suchkov, A., Crook, I., Tibitche, Z., Lizzi, J. and Subbu, R., "NextGen collaborative air traffic management solutions", In AIAA Guidance, Navigation and Control Conference and Exhibit, (2008), 1–12.

18. Bicchi, A. and Pallottino, L., "On optimal cooperative conflict resolution for air traffic management systems", *IEEE Transactions on Intelligent Transportation Systems*, Vol. 1, No. 4, (2000), 221–231.

19. Liu, W. and Hwang, I., "Probabilistic aircraft midair conflict resolution using stochastic optimal control", *IEEE Transactions on Intelligent Transportation Systems*, Vol. 15, No. 1, (2013), 37–46.

20. Zhu, L., Cheng, X. and Yuan, F. G., "A 3D collision avoidance strategy for UAV with physical constraints", *Measurement*, Vol. 77, (2016), 40–49.

21. Holt, J., Biaz, S. and Aji, C. A., "Comparison of unmanned aerial system collision avoidance algorithms in a simulated environment", *Journal of Guidance, Control, and Dynamics*, Vol. 36, No. 3, (2013), 881–883.

22. Omer, J., "A space-discretized mixed-integer linear model for air-conflict resolution with speed and heading maneuvers", *Computers & Operations Research*, Vol. 58, (2015), 75–86.

23. Alonso-Ayuso, A., Escudero, L.F. and Martín-Campo, F. J., "On modeling the air traffic control coordination in the collision avoidance problem by mixed integer linear optimization", *Annals of Operations Research*, Vol. 222, No. 1, (2014), 89–105.

24. Cafieri, S. and Rey, D., "Maximizing the number of conflict-free aircraft using mixed-integer nonlinear programming", *Computers & Operations Research*, Vol. 80, (2017), 147–158.

25. Patel, R.B. and Goulart, P. J., "Trajectory generation for aircraft avoidance maneuvers using online optimization", *Journal of Guidance, Control, and Dynamics*, Vol. 34, No. 1, (2011), 218–230.

26. Raghunathan, A.U., Gopal, V., Subramanian, D., Biegler, L.T. and

Samad, T., "Dynamic optimization strategies for three-dimensional conflict resolution of multiple aircraft", *Journal of Guidance, Control, and Dynamics*, Vol. 27, No. 4, (2004), 586–594.

27. Guo, T., Li, J., Baoyin, H. and Jiang, F., "Pseudospectral methods for trajectory optimization with interior point constraints: Verification and applications", *IEEE Transactions on Aerospace and Electronic Systems*, Vol. 49, No. 3, (2013), 2005–2017.

28. Ross, I.M. and Karpenko, M., "A review of pseudospectral optimal control: From theory to flight", *Annual Reviews in Control*, Vol. 36, No. 2, (2012), 182–197.

29. Dutykh, D., A brief introduction to pseudo-spectral methods: application to diffusion problems, HAL Id: cel-01256472, https://cel.archives-ouvertes.fr/cel-01256472v2, (2016).

30. Garg, D., Patterson, M., Hager, W., Rao, A., Benson, D. and Huntington, G., An overview of three pseudospectral methods for the numerical solution of optimal control problems, HAL Id: hal-01615132, https://hal.archives-ouvertes.fr/hal-01615132, (2017).

31. Mortazavi, H., Salahshoor, A. and Hamidi, H., "Designing and modeling a control system for aircraft in the presence of wind disturbance", *International Journal of Engineering - Transaction C: Aspects*, Vol. 30, No. 12, (2017), 1856–1862.

32. Menon, P. K. A., "Short-range nonlinear feedback strategies for aircraft pursuit-evasion", *Journal of Guidance, Control, and Dynamics*, Vol. 12, No. 1, (1989), 27–32.

33. Wang, J. and Xin, M., "Integrated optimal formation control of multiple unmanned aerial vehicles", *IEEE Transactions on Control Systems Technology*, Vol. 21, No. 5, (2012), 1731–1744.

34. Redding, J., Amin, J., Boskovic, J., Kang, Y., Hedrick, K., Howlett, J. and Poll, S., "A real-time obstacle detection and reactive path planning system for autonomous small-scale helicopters", In AIAA Guidance, Navigation and Control Conferenc and Exhibit, (2007), 1–22.

35. Yang, X., Alvarez, L.M. and Bruggemann, T., "A 3D collision avoidance strategy for UAVs in a non-cooperative environment", *Journal of Intelligent & Robotic Systems*, Vol. 70, No. 1–4, (2013), 315–327.

36. Pham, H., Smolka, S.A., Stoller, S.D., Phan, D. and Yang, J., "A survey on unmanned aerial vehicle collision avoidance systems", *arXiv:1508.07723*, (2015), 1–10.

37. Chen, W., Chen, J., Shao, Z. and Biegler, L. T., "Three-dimensional aircraft conflict resolution based on smoothing methods", *Journal of Guidance, Control, and Dynamics*, Vol. 39, No. 7, (2016), 1481–1490.

38. Betts, J. T., "Survey of numerical methods for trajectory optimization", *Journal of Guidance, Control, and Dynamics*, Vol. 21, No. 2, (1998), 193–207.

39. Lilium Jet, June 2016. [Online]. Available: https://www.aerospace-technology.com/projects/lilium-jet

---

Persian Abstract

چکیده

در این مقاله یک روش جدید برای مسیریابی متمرکز برای چند هواپیما با در نظر گرفتن قوانین پرواز در ارتفاع کم در فضای پروازی با تعداد زیادی موانع ارائه می‌شود. این موضوع بصورت یک مسئله کنترل بهینه مقید غیرخطی مطرح می‌شود. توابع کمترین زمان و کمترین انرژی بعنوان توابع هزینه، محدودیت بیشترین سرعت و بیشترین توان بعنوان قیود حالت و کنترل اعمال می‌شوند. برای این منظور با استفاده از روش مستقیم شبه طیفی که یک روش متداول و سریع درحل مسائل کنترل بهینه مقید است؛ این مسئله مورد بررسی قرار می‌گیرد. برای مدلسازی مسئله از مدل حرکت سه درجه آزادی با فرض جرم ثابت و با اعمال محدودیت‌های واقعی عملکرد و کنترل استفاده می‌شود. موانع ثابت بصورت اشکال مختلف با ترکیب چند کره با شعاع‌های مختلف در فضای سه بعدی مدلسازی می‌گردند. همچنین موانع متحرک، کره‌هایی با شعاع مشخص و سرعت ثابت فرض می‌شوند. به منظور صحه‌سنجی، با استفاده از چهار مطالعه موردی متفاوت با تعداد هواپیماهای مختلف روش پیشنهادی مورد مطالعه قرار می‌گیرد و مسیرهای پروازی بدون تداخل از میان موانع ثابت و متحرک محاسبه می‌گردند.